Estimation of Mean and Median Frequency from synthetic sEMG signals: effects of different spectral shapes and noise on estimation methods.

Giovanni Corvini[1], Carmen D'Anna, Silvia Conforto

Department of Engineering, Roma Tre University, Via Vito Volterra 62, 00146 Rome, Italy

Abstract

The detection of electrical signs of muscle fatigue passes through the choice of appropriate spectral estimation techniques for the extraction of parameters such as Mean and Median Frequency from surface myoelectric signals. Unfortunately, despite the huge number of contributions using various spectral techniques to process signals recorded in fatiguing protocols, there is no agreement on the method that works best, and, to our knowledge, the performance of the estimation techniques has been evaluated only on a limited range of spectral shapes (i.e., limited range of Mean and Median Frequency). To study the fatigue phenomenon, it is important to consider the range of variation of the spectral parameters and then the different shapes assumed by the signal spectrum. To this aim this works will explore the performance of the most widespread spectral estimation techniques when applied on synthetic myoelectric signals characterized by different spectral shapes associated with different Mean and Median frequency within the signal band. Also, different noise conditions have been used to test the following spectral estimation techniques: a) indirect technique by the estimation of the autocorrelation function of the signal; b) direct technique by the Welch estimation method with special attention to the different window functions that can be used to segment the signal; c) Burg autoregressive approach with special attention to the model order. The main result, after assessing that Burg's approach outperforms all the other techniques for all the examined conditions, outlines that the model's order, whose range is between the 8^{th} and the 12^{th}, depends on the spectral shape and is critical for the estimation of the Median Frequency of the signal. This partially overwrites previous results of the literature and provides the useful recommendation to choose, among the spectral estimation techniques aimed at detecting the electrical signs of muscle fatigue, those that prove to be more adaptive with respect to the dynamics of the fatigue process.

Keywords

PSD estimation, Mean Frequency, Median Frequency, Welch method, AR model, simulated sEMG signals.

1 G. Corvini, corresponding author, email address: giovanni.corvini@uniroma3.it

1. Introduction

Surface electromyography (sEMG) is one of the most powerful tools to non-invasively obtain valuable information from muscles and extract several features to be used in a variety of contexts and applications (e.g., assessment, classification, control) [1][2]. Among all the possible features that can be extracted [3][4], Mean (MNF) and Median Frequency (MDF) are the traditional ones to assess myoelectric manifestation of muscle fatigue [5][6]. Since these parameters are extracted from a frequency representation of the sEMG signal, their quality depends on the characteristic of the estimation technique chosen for the spectral representation and must be assessed by using bias and variance [7]. This estimation problem is not new, and several simulation studies have been published some years ago to address this topic [8][9][10]. The performance of the spectral estimation techniques, however, can change depending on the implementation: in fact, different settings are needed for the estimation, such as the length and the shape of the window used to segment the signal [8][11], the number of segments used for the estimation [11], the order of the model in the parametric approaches [11][12]. These settings are factors that differently affect the performance depending on the characteristics of the signal analyzed. In this line is the work presented by Farina et al. [12], where periodogram and autoregressive approaches are compared with respect the estimation of MNF and MDF on simulated signals. Also, the effect of the window length has been tested in that study and this factor of influence has been also assessed recently in [13][14] [15]. Farina [12] demonstrated that autoregressive outperforms periodogram and provides comparable performance for model orders larger than ten. However, neither the Farina's work nor other studies, to our knowledge, tested how implementation settings can have different influences on MNF and MDF estimation in signals with different spectral shapes.

In this work, we want to address this issue by analyzing four different shapes of the spectrum, simulating plausible physiological condition of a generic muscle (from initial state of a contraction to severe muscle fatigue). In fact, recent works in different scientific areas found substantial decreases of MDF [16][17][18][19] and MNF [18][19] caused by the presence of muscular fatigue, showing the feasibility of encountering very low values in spectral parameters, which have not been considered in previous comparison of estimation methods. For this reason, the scope of this work was to evaluate the performance of the most common estimation methods [20] considering four different frequency contents of synthetic sEMG signals. These signals were generated considering different Mean and Median frequency values - and thus different spectrum shapes - and different noise conditions and have been used as testing set of some spectral estimation techniques such as: a) indirect technique by the estimation of the autocorrelation function of the signal; b) direct technique by the Welch estimation method with special attention to the different window functions that can be used to segment the signal; c) Burg autoregressive approach with special attention to the model order.

The error provided by the different techniques in the different conditions has been used as criterion to determine the most robust estimation approach with respect to noise and to both the content and the shape of the spectrum that discriminate different scenarios of the fatiguing phenomenon.

2. Methods

2.1 Simulation procedure

A dataset of stationary sEMG signals with different ideal Mean and Median Frequency values was generated. Each realization was synthetized using the sEMG model proposed by Stulen and De Luca [21], that shapes a zero mean white process with unit variance through a shaping filter to generate:

$$P_{xx}(f) = \frac{k^2 f_h^4 f^2}{(f^2 + f_l^2)(f^2 + f_h^2)^2} \qquad 1)$$

where P_{xx} is the ideal PSD, k^2 is a scaling factor, f is the frequency that ranges from zero to half of the sampling frequency ($f_s/2$) to consider only the positive part of the spectrum, while f_l and f_h are the low and high cut-off frequencies, respectively. In this work, we set k^2=1 and $f_s=1024Hz$. The duration of the signals was set to T=250ms. This choice was justified by the interest in using these spectral techniques in applications that could possibly work in pseudo real-time. Moreover, according to [12], this window length (250ms) resulted to be the minimum length that no introduce high variance and bias in the estimation. A total of 4 batches, each one comprising 1000 signals, have been generated by varying the pair of the cut-off frequencies (f_l and f_h) in the sEMG model to simulate different physiological state of the muscle (rest, initial fatigue, fatigue, severe fatigue). The pairs of cut-off frequencies were chosen according to the example presented in [12]:

a. $f_l=30$-$f_h=60$, producing an ideal MNF=59.68Hz and an ideal MDF=46.88Hz
b. $f_l=40$-$f_h=100$, producing an ideal MNF=91.85Hz and an ideal MDF=73.27Hz
c. $f_l=60$-$f_h=120$, producing an ideal MNF=114.94Hz and an ideal MDF=94Hz
d. $f_l=50$-$f_h=150$ producing an ideal MNF=126.61Hz and an ideal MDF=103.64Hz

We will use "cut-off" as a factor with four levels to indicate the location in frequency of the power content of the signals in the statistical analysis. Then, we have generated a further random 1000 realizations of white Gaussian noise with T=250ms and added them to the sEMG signals to simulate typical SNR conditions (5, 10, 15 and 20dB) as in [22]. The resulting myoelectric signals, 16000 in total, have the following form:

$$x_n = \sum_{i=0}^{N} w_n\, h_{n-i} + n_n \qquad \textit{with } n = 0, 1, \ldots, N \qquad 2)$$

where N is the number of samples, w_n is the white gaussian noise to be modulated as input of the filter, h_n is the shaping filter and n_n is an independent realization of white gaussian noise. The two noise processes w_n and n_n are assumed to be uncorrelated with each other. The filter h_n has been obtained by taking the real part of the inverse Fourier Transform of the amplitude spectrum (square root of $P_{xx}(f)$), whose phase was reconstructed as the imaginary part in the Hilbert transformation of the logarithm of the magnitude.

2.2 Mean and Median Frequency

For the analysis, we have computed the Mean and Median Frequency. MNF is an average frequency which is calculated according to the following equation:

$$MNF = \frac{\sum_{j=1}^{L} P_j f_j}{\sum_{j=1}^{L} P_j} \quad 3)$$

where P_j is the *j-th* line of the Power spectrum, f_j is the *j-th* frequency and L is the line at the highest frequency of the signal bandwidth, which depends on the time duration and the sampling frequency. Conversely, the Median Frequency is the frequency at which the sEMG Power spectrum is exactly divided into two regions equivalent in power [5], and it can be computed as:

$$\sum_{j=1}^{MDF} P_j = \sum_{j=MDF}^{L} P_j = \frac{1}{2}\sum_{j=1}^{L} P_j \quad 4)$$

where P_j, f_j and L are defined as before.
MNF and MDF coincide if the spectrum is symmetric with respect to its center line while they differ if the spectrum is skewed as in this case, where the shaping filter offered a skewed shape.

2.3 Techniques to estimate and compute the Power Spectral Density

In the following, all the analyzed estimation techniques (implemented in MATLAB) are described. These techniques are grouped in two categories: non-parametric, which estimate the PSD directly or indirectly from the data, and parametric that aims to estimate parameters to develop a model from which computing the PSD. The PSD could be computed as the square module of the Fast Fourier Transform (FFT) if we are dealing with continuous-time signals of infinite duration, as stated by the Wiener-Kintchine theorem [23]. Unfortunately, this condition cannot be met in the real world because signals are finite, thus several techniques have been developed to estimate the PSD or a model able to compute the PSD.

2.3.1 Non-parametric estimation

Since a real sEMG signal is finite in time, we can deal with an ideal infinite signal limited in duration by multiplying it to a window function (with the same length as the original length of the real signal) to extract a specific portion of interest of the signal and then apply the FFT. This operation is called Periodogram, and it can be implemented according to the formula:

$$\hat{P}_{xx}(k) = \frac{1}{N}\left|\sum_{n=0}^{N-1} w_n x_n e^{-j2\pi\frac{kn}{N}}\right|^2 \quad 5)$$

where N is the number of samples, w_n is the rectangular window function and x_n is the signal. By using this method, the PSD results to be an estimate, from which we computed the MNF and MDF. Unfortunately, the Periodogram method is inconsistent because its variance does not tend to zero as the number of signal samples increases. Therefore, some modifications of this method have been proposed in the literature (like the method of Bartlett [24] or Welch [25]) to solve this problem.

The Welch's method is an extended version of the Periodogram aiming at improving the estimate of the Power spectrum by reducing the variance of the estimate, solving the inconsistency problem presented before. To achieve this goal, this method divides the input signal of N samples into S segments each consisting of $k=N/S$ samples, computes the periodogram for each segment and then averages the result. To extract a segment, the signal was multiplied by a window function with length equal to a percentage of the original signal length, and this window function was moved along the signal with a partial overlap. Thus, we extracted several segments and computed the PSD with Welch method as:

$$\hat{P}_{xx}(f) = \frac{1}{S}\sum_{i=1}^{S} I_k^{(i)}(f) \quad 6)$$

where $I_k^{(i)}$ is the *i-th* periodogram computed on k samples as in equation 5, and S is the number of segments on which the periodogram has been computed. In our work, signals have been divided into a total of 8 segments (S=8) considering an overlap of 50% of the length of the segment. To evaluate the performance of different window functions, w_n in equation 5 with took expression of the corresponding window function (e.g., Bartlett, Kaiser, Tukey, etc.). A list of all mathematical formulations of the windows can be found in Appendix A.

Another way to generate the PSD is an indirect method, that is the FFT of the Autocorrelation of the signal. In this case (i.e., real signals) the Autocorrelation function cannot be computed but must be estimated resulting, in turn, in PSD estimation given by:

$$\hat{P}_{xx}(k) = \sum_{n=0}^{N-1} \hat{R}_{xx}(m) e^{-j2\pi\frac{kn}{N}} \quad 7)$$

where $\hat{R}_{xx}$ is the estimate of the Autocorrelation function. We used the unbiased version of this estimator, defined as:

$$\hat{R}_{xx}(m) = \frac{1}{N-m} \sum_{n=0}^{N-m-1} x_{n+m} x_n^* \qquad \textit{with } m = 0, 1, \ldots, M \quad 8)$$

where x_{n+m} is the *n-th* sample of the signal at lag *m* and x_n^* is the *n-th* complex conjugate sample. In the MATLAB implementation, the autocorrelation was limited in a range defined by the built-in *maxlag* variable that has been set to half of the length of the signal. We will use the acronym AC to identify the unbiased version in the results section.

2.3.2 Parametric estimation

Another approach for PSD estimation is called parametric or model based. This method assumes that the signal is a realization of a stochastic process that can be described by a mathematical model, which acts as a filter on an input sequence of white gaussian noise. Thus, the PSD estimation problem is transformed in the estimation of the parameters of the model. One of the most powerful models is the so-called ARMA (AutoRegressive Moving Average) model, in which each sample x_n of the signal can be described as a linear combination of p past outputs and $q+1$ present and past inputs. We focused only on the AutoRegressive model using the Burg's method [26], which estimates the reflection coefficient a_{pp} from past samples (measured data) to estimate the future samples of the signal as:

$$\hat{x}(n) = -\sum_{l=1}^{p} a_{pl}\, x_{n-l} \qquad 9)$$

where a_{pl} are the prediction coefficients computed for the model order p through the iterative Levinson Durbin algorithm. The resulting PSD is obtained as following:

$$P_{xx}(f) = \frac{\sigma_l^2}{\left|1 + \sum_{l=1}^{p} a_{pl} e^{-j2\pi l \frac{kn}{N}}\right|^2} \qquad 10)$$

where σ_l^2 is the total error. As a result, the Burg methods aims to simultaneously minimize through the Least Mean Square Error (LSME) criterion the total error, which is the sum of the forward e_l and the backward b_l prediction errors and must be computed for each value of the order l of the model ($l=1, 2, \ldots, p$).

$$\sigma_l^2 = \min_\alpha \left\{ E_l = \sum_{n=l}^{N-1} |e_l(n)|^2 + \sum_{n=l}^{N-1} |b_l(n)|^2 \right\} \qquad 11)$$

Unfortunately, by increasing the order of the AR model, and thus increasing the number of the parameters to be estimated, the computational complexity increased as well. Consequently, under similar performance in the results, the minimum order must be preferred. In the following, we use the term PSD estimation, but it is worth noting that when we refer to the Autoregressive method, we estimated the parameters of the model from which the PSD was computed, instead of estimated.

2.4 Statistical Analysis

The statistical analysis was performed for both frequency parameters (mean and median frequency), by evaluating the Mean Absolute Error (MAE) following the equation:

$$MAE = \frac{1}{C}\sum_{c=1}^{C} y_d - y_c \qquad \textit{with } c = 0, 1, \ldots, 1000 \qquad 11)$$

where y_d is the MNF or MDF ideal value, y_c is the computed value from the estimation technique and C is the total number of synthetic signals. For both parameters descriptive statistics was calculated (mean and standard deviation). We started from a global analysis investigating the interactions between three factors by performing a three-way ANalysis Of VAriance (ANOVA). Subsequently, to investigate the interactions between only two factors, we fixed one factor analyzing all its levels. To this scope, we computed a two-way ANOVA (for each level of the fixed factor). Finally, when two-way ANOVA was significant, we fixed another factor and performed a one-way ANOVA to assess the effect of the remaining factor (for each level of the second fixed factor). If also one-way ANOVA resulted significant, the Tukey's HSD post-hoc test was applied to find out the differences between the levels of the single factor. The statistical analysis was carried out using the software R [27] and the significance level was set to: *p<0.05, **p<0.01, ***p<0.001. The details of statistical analysis are reported in the following subparagraphs.

2.4.1 Comparison of window functions for Welch method

For this analysis, a 3-ways ANOVA was performed by using the following factors:

- *Window*, 16 levels (Bartlett, Barthann, Blackman, Blackmanharris, Chebyshev, Flattop, Gaussian, Hamming, Hann, Kaiser, Nuttal, Parzen, Rectangular, Taylor, Triangular, Tukey)
- *SNR*, 4 levels (5dB, 10dB, 15dB, 20dB)
- *Cut-off*, 4 levels (30-60, 40-100, 60-120, 50-150)

2.4.2 Comparison of orders for Burg method

For this analysis, the following factors have been used in the 3-ways ANOVA:

- *Order*, 10 levels (from 6th to 15th order)
- *SNR*, 4 levels (5dB, 10dB, 15dB, 20dB)
- *Cut-off*, 4 levels (30-60, 40-100, 60-120, 50-150)

2.4.3 Method comparison

For this analysis, a 3-ways ANOVA was performed by using the following factors:

- *Method*, 4 levels (Welch, AC, 8th order of Burg, 12th order of Burg)
- *SNR*, 4 levels (5dB, 10dB, 15dB, 20dB)
- *Cut-off*, 4 levels (30-60, 40-100, 60-120, 50-150)

A summary of the entire work is summarized in figure 1 highlighting the three steps: generation of signals, processing with different estimation methods and statistical analyses.

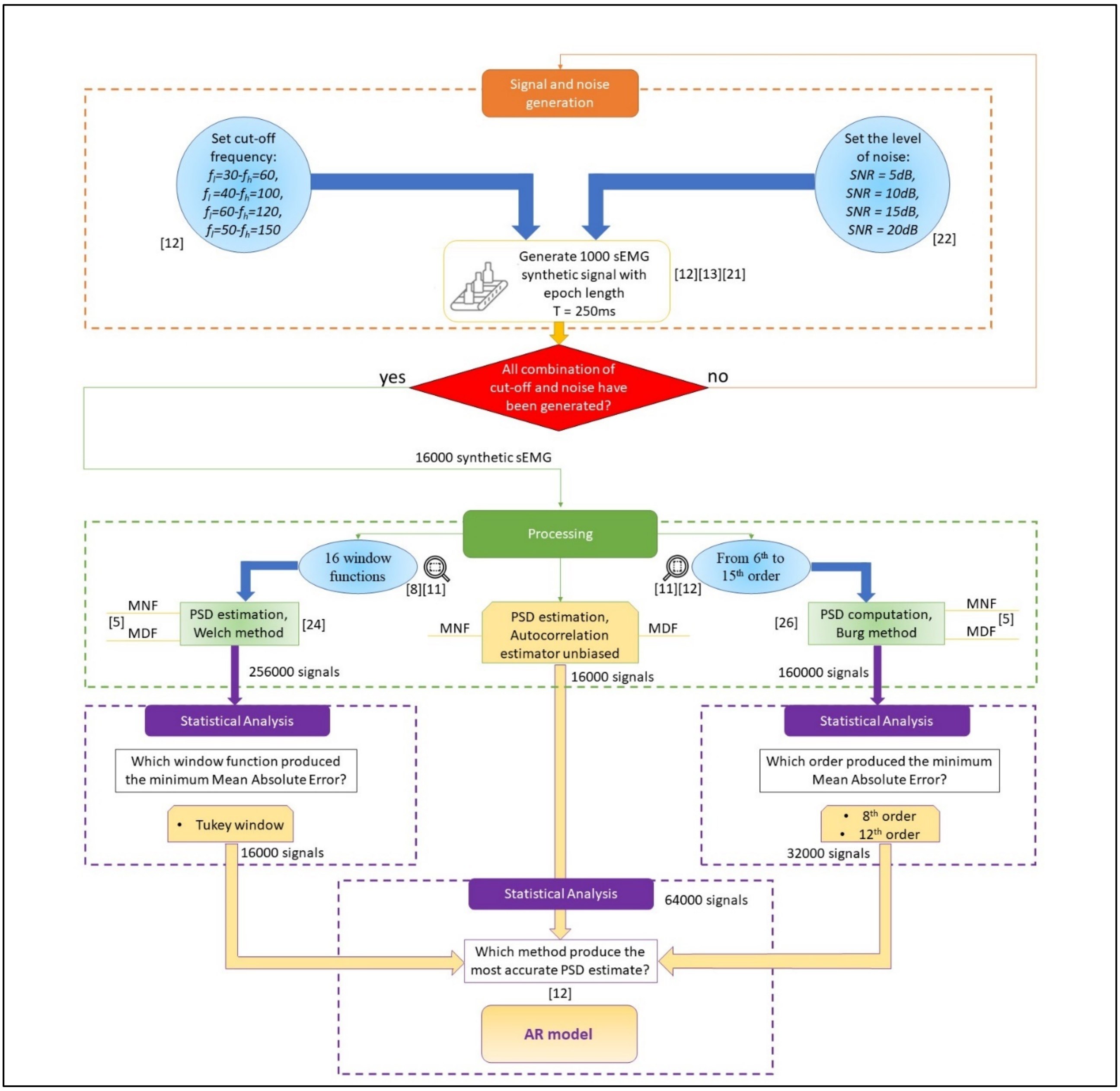

Figure 1 Graphical flowchart summarizing the entire work

3. Results

3.1 Window functions in Welch implementation

For both MNF and MDF, three-ways ANOVA showed no significance in the interaction effect among *SNR*, *window*, and *cut-off*. By fixing the *SNR*, two-way ANOVA was computed, whose results are showed in table 1. For both spectral parameters, the interaction effect between *cut-off* and *window* was significant only for high level of SNR≥15dB ($p<0.001$). Finally, one-way ANOVA tests (each one computed for each level of *cut-off*) were performed on the *window* factor and all of them showed significance for both MNF and MDF ($p<0.001$).

Regarding the MNF, the post-hoc tests revealed that *Tukey* window always produced the minimum error but, the significance of the difference with the other windows depended on the level of SNR. In general, for high level of SNR (SNR=15 and 20dB), the difference between *Tukey* and all the other windows was significant ($p<0.05$) except with respect to the following windows: *Taylor*, *Triangular*, *Bartlett* and *Hamming*. By decreasing the SNR (greater level of noise), the difference among the windows started to be not significant, until it was not significant among any window at SNR equal to 5dB. For greater cut-off frequencies ($f_l=60$-$f_h=120$ and $f_l=50$-$f_h=150$), the same behavior was encountered: *Tukey* window always produced the minimum error when SNR≥15dB, and the difference with respect to all the other windows was significant except for *Taylor*, *Kaiser*, *Rectangular*, *Triangular*, and *Bartlett*. As before, the difference between *Tukey* and all the other windows failed to be significant as the SNR decreased.

Table 1 Two-way ANOVA test results: F-statistics and p-values for Mean Absolute Error computed for MNF. Each test was performed fixing one SNR level while considering cut-off and window function as main factors. The level of significance was set to *p<0.05, **p<0.01 and ***p<0.001.

	SNR=5dB		***SNR=10dB***		***SNR=15dB***		***SNR=20dB***	
MNF	F-statistic	p-value	F-statistic	p-value	F-statistic	p-value	F-statistic	p-value
Cut-off	7.1e+03	0***	1.5e+03	0***	1.01	0.384	264.05	0***
Window	11.80	0***	31.05	0***	80.40	0***	112.69	0***
Cut-off*window	0.49	0.998	0.78	0.856	3.12	0***	2.785	0***
MDF	F-statistic	p-value	F-statistic	p-value	F-statistic	p-value	F-statistic	p-value
Cut-off	534.66	0***	787.86	0***	944.40	0***	999.34	0***
Window	52.00	0***	79.78	0***	85.04	0***	84.53	0***
Cut-off*window	0.21	1	1.002	0.46	1.411	0.03*	1.55	0.01*

Regarding the MDF, similar results were found. Post-hoc tests showed that *Taylor* window produced the minimum error when cut-off was $f_l=30$-$f_h=60$ and *SNR=5dB*, even if the difference with *Tukey* was not significant. For all the other levels of *SNR, Tukey* window always produced the minimum error. When analyzing all the other *cut-off* ($f_l=40$-$f_h=100$, $f_l=50$-$f_h=150$, $f_l=60$-$f_h=120$), *Tukey* window always generated the minimum error (SNR≥5dB), but the difference was statistically significant ($p<0.001$) only if compared to the following window functions: *Blackman*, *Blackmanharris*, *Chebyshev*, *Flattop, Nuttal* and *Parzen*.

Since the *Tukey* window produced the minimum error in most of the cases, this window was used in the method comparison.

3.2 Order of Burg method

For the AR model, we visually inspected the behavior of the PSD computed with thirty different orders, as exemplified in figure 2. Since the AR model was not able to approximate the PSD shape with less than 6 parameters and started to introduce a high level of noise with more than 15 parameters, to simplify the statistical analysis, we studied only ten orders starting from the 6th up to the 15th order. When the ideal power of the spectrum was concentrated at low frequencies (f_l*=30-*f_h*=60*, that is MDF_{ideal}=46.88Hz), many parameters were necessary to correctly shape the PSD (figure 2 on the left). PSD shape of the signal began to be well approximated from the 12th order until the 20th, after which the model started to overfit the PSD by introducing noise (i.e., more peaks, like those in light blue with Amplitude equal to 0.4). Contrarily, when the power content was found at higher frequencies (MDFideal=94Hz), as in figure 2 on the right, the PSD shape was well-approximated with a few parameters (ranging from 6-7 to 12) before starting to introduce noise. This was reflected on the errors in MNF and MDF computation.

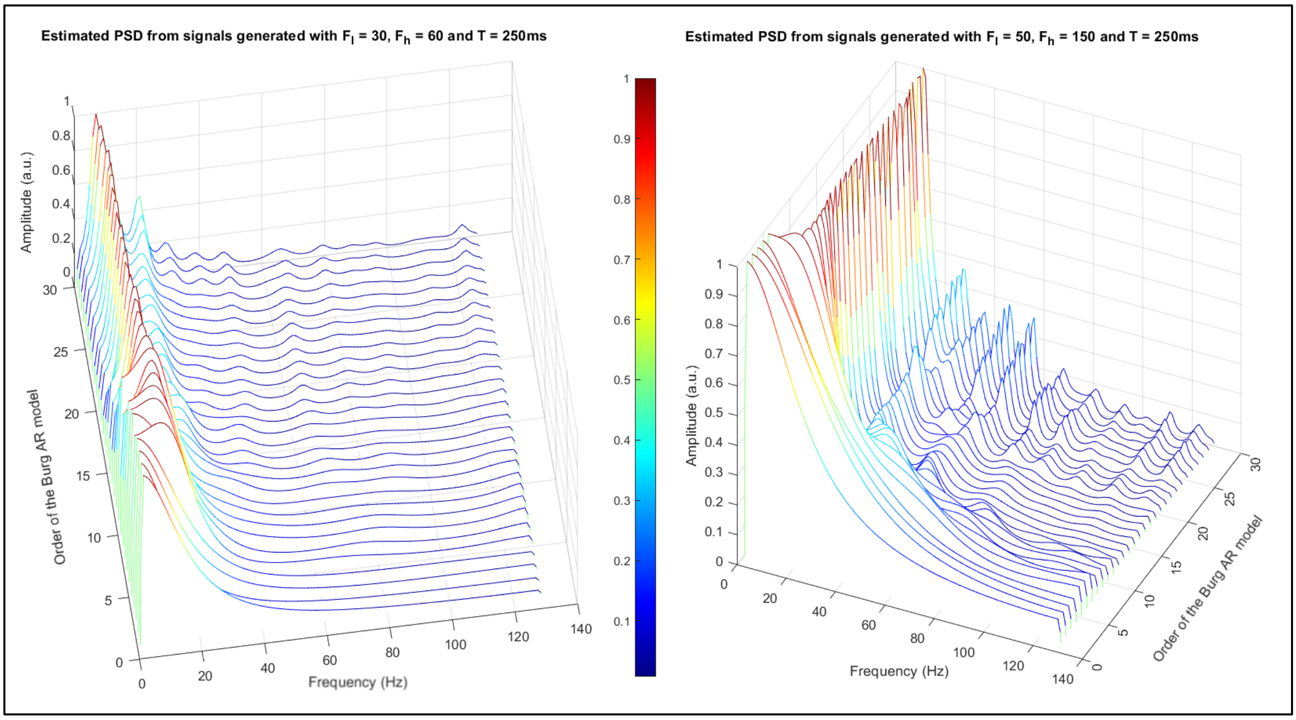

Figure 2 Estimated Power Spectrum Densities (PSDs) from 30 orders of the AR model at SNR=5dB. On the left, the PSDs were estimated from signals generated by cut off frequencies f_l*=30-*f_h*=60*. It can be noticed that the PSD started from half of its maximum at the first orders of the model and the ideal bell shape of the PSD is reached from the 12th order onwards. A great variance in the PSD shape, identified by the presence of more than one peak, started to be present around the 28th-30th order. On the right, the PSDs were estimated from signals that have been generated with cut-off frequencies f_l*=60-*f_h*=120*. Here the ideal bell shape of the PSD is reached at the 6th order, and noise can be seen from the 12th order onwards.

Regarding the MNF, three-way ANOVA indicated that there was not a statistically significant interaction among SNR, order, and cut-off frequency. A two-way ANOVA showed no significance in the interaction between order and SNR, and order and cut-off frequency. Therefore, one-way ANOVA was performed on the order (averaging across all the levels of SNR), and it showed significance ($p<0.001$). Post-hoc test revealed that the difference among the 6th and the 9th order and higher, the 7th and the 12th and higher, and the 8th and the 15th order were significant ($p<0.01$). Overall, by increasing the SNR, smaller errors were found in MNF computations. The minimum error was generated by the 6th order in each examined case (for each level of SNR and for each level of cut-off frequency).

Different results have been found in the analysis of MDF, as shown in figure 3. In fact, three-way ANOVA showed that there was a statistically significant interaction effect ($p<0.001$) among the three factors: SNR, order, and cut-off frequency. By fixing the cut-off to $f_l=30$-$f_h=60$, two-way ANOVA indicated a significant interaction ($p<0.001$) between SNR and order. When SNR was 5 and 10dB, one-way ANOVA performed on the *order* showed that the minimum error was found at the 13th. As the SNR increased to 15 and 20dB, the minimum number of estimated parameters decreased to 12th and 11th, respectively. In general, MAE was significant between an order and two and more subsequent ones (i.d, 6th and the 7th orders were different ($p<0.05$) from the 9th to 15th orders, the 8th order was different from 10th to 15th, and the 9th order was different from 11th to 15th). For cut-off equal to $f_l=40$-$f_h=100$, the minimum error was produced by the 9th order in presence of high noise (SNR=5 and 10dB), reaching the 8th order, which was statistically different from the 11th to 15th order, when SNR=15 and 20dB. For cut-off equal to $f_l=60$-$f_h=120$ or $f_l=50$-$f_h=150$, the interaction effect between *SNR* and *order* was not significant. One way ANOVA tests were performed on the *order* factor and resulted significant ($p<0.001$). Post-hoc tests showed that the 7th order produced the minimum error, and the difference was statistically significant ($p<0.001$) with respect to all the other orders except for the 6th (and 8th when $f_l=60$-$f_h=120$). Since there was not an optimal order because it depended on the location of the power content and on the amount of noise in signals, we empirically selected two different orders (8th and 12th) to be compared with other methods.

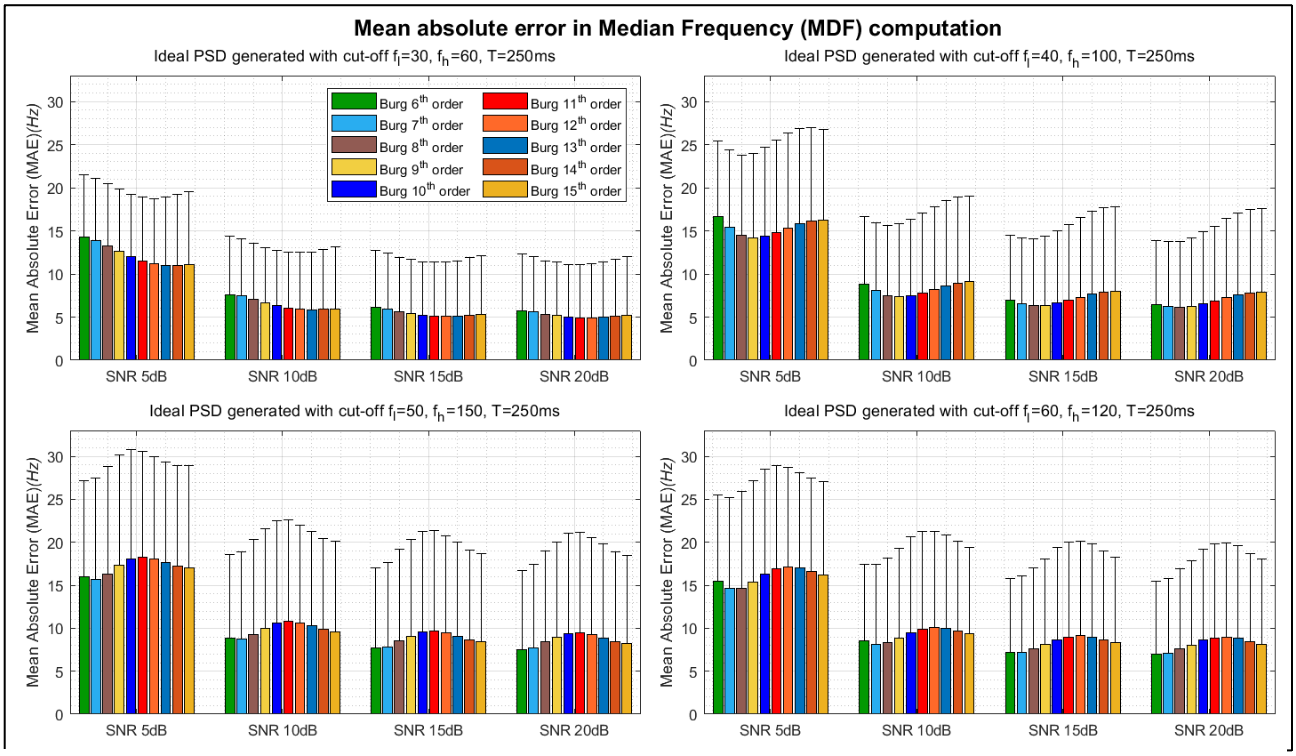

Figure 3 Mean Absolute Error (MAE) computed on Median Frequency computation (MDF). The ideal PSD were generated with four cut-off frequencies, and errors were analysed at four different level of SNR. The duration of the signals was T=250ms. The power content in frequency (represented by the cut-off) and the SNR had a statistically significant interaction effect ($p<0.001$), which influence the choice of the optimal order of the autoregressive model.

3.3 All methods comparison

For the global comparison, Welch method (*Tukey* window), unbiased Autocorrelation, 8^{th} and 12^{th} order of autoregressive model (Burg method) were analyzed. Overall, as expected, by increasing SNR, the Mean Absolute Error decreased in both MNF and MDF computations for each method. In most of the examined cases, the AR model, in particular the 8^{th} order, was able to better approximate a PSD shape to the ideal one, resulting in a more accurate PSD estimation with respect to the other methods.

Table 2 Three-way ANOVA test results: F-statistics and p-values for MAE computed for MNF and MDF considering SNR, method, and cut-off as main factors. The level of significance was set to *p<0.05, **p<0.01 and ***p<0.001. In red the non-significant p-value.

	MNF		*MDF*	
	F-statistic	p-value	F-statistic	p-value
SNR	96260.82	< 2e-16 ***	4837.69	<2e-16 ***
Method	793.84	< 2e-16 ***	328.12	<2e-16 ***
Cut-off	2364.32	< 2e-16 ***	820.56	<2e-16 ***
*SNR*method*	12.75	< 2e-16 ***	15.05	<2e-16 ***
*SNR*cut-off*	1236.76	< 2e-16 ***	10.42	<2e-16 ***
*Method*cut-off*	2.64	0.0046 **	21.61	<2e-16 ***
*SNR*method*cutoff*	1.08	0.34	1.68	0.0149*

Three-way ANOVA is shown in table 2, reporting the value of the F-statistic and the p-value of the interaction effects of settings on the computation of MNF and MDF.

3.3.1 Effect on Mean Frequency

Three-way ANOVA test indicated that there was not a significant interaction effect among *SNR*, *cut-off,* and *methods*. Two-way ANOVA tests (four tests, one for each level of *SNR*) exhibited a significant effect ($p<0.001$) in the interaction between *cut-off* and *method* only when SNR was greater than 10dB, as exemplified in table 2. Therefore, one-way ANOVA tests were performed on the methods (four tests, one for each level of *cut-off*) resulting significant ($p<0.001$). Post-hoc tests identified the significant differences between each pair of methods. For cut-off equal to $f_l=30$-$f_h=60$, the minimum error was produced by the *8th order* of the autoregressive model but the difference with the *12th order* was not significant, while it was significant ($p<0.05$) if compared with *Welch* and *AC* for SNR less than 20dB. When SNR=20dB, the results obtained by the *8th order, 12th order,* and *Welch* were very similar (difference was not significant) and could be utilized interchangeably. For all the other cut-off frequencies, that means MNF values ranging from 70 to 105Hz, the minimum error was generated by the *8th order* regardless of the level of SNR, although the difference was significant only with respect to *AC* ($p<0.001$) and not with *12th order* and *Welch*.

Finally, only for low level of SNR (5 and 10dB), a single method produced different errors according to the cut-off frequency used for generating the signals; that means that the same estimation method produced an error in evaluating a frequency content of a signal, and consequently a specific spectral shape, that is significantly different ($p<0.001$) from the error computed by evaluating a different spectral shape. These results have been found for each single method. In our study, Burg 8^{th} order showed a huge MAE with a decreasing trend when MNF increased: as an example, MAE=48Hz when MNF=59.68Hz and MAE=32Hz when MNF=114.94Hz. When the SNR is higher (15 and 20dB) the error substantially decreased and the differences generated by the same method across cut-off frequencies, as well as their significance, disappeared. Mean Absolute Errors computed by different cut-off frequencies and for each level of SNR, are shown in figure 4.

Table 3 Two-way ANOVA test results: F-statistics and p-values for Mean Absolute Error computed for MNF. Each test was performed fixing one cut-off while considering SNR and method as main factors. The level of significance was set to *p<0.05, **p<0.01 and ***p<0.001.t

	SNR=5dB		***SNR=10dB***		***SNR=15dB***		***SNR=20dB***	
	F-statistic	p-value	F-statistic	p-value	F-statistic	p-value	F-statistic	p-value
Cut-off	3485.20	0***	623.28	0***	6.59	0***	43.49	0***
Method	151.07	0***	267.93	0***	269.51	0***	154.99	0***
Cut-off*method	0.397	0.93	0.34	0.95	3.83	0***	3.66	0***

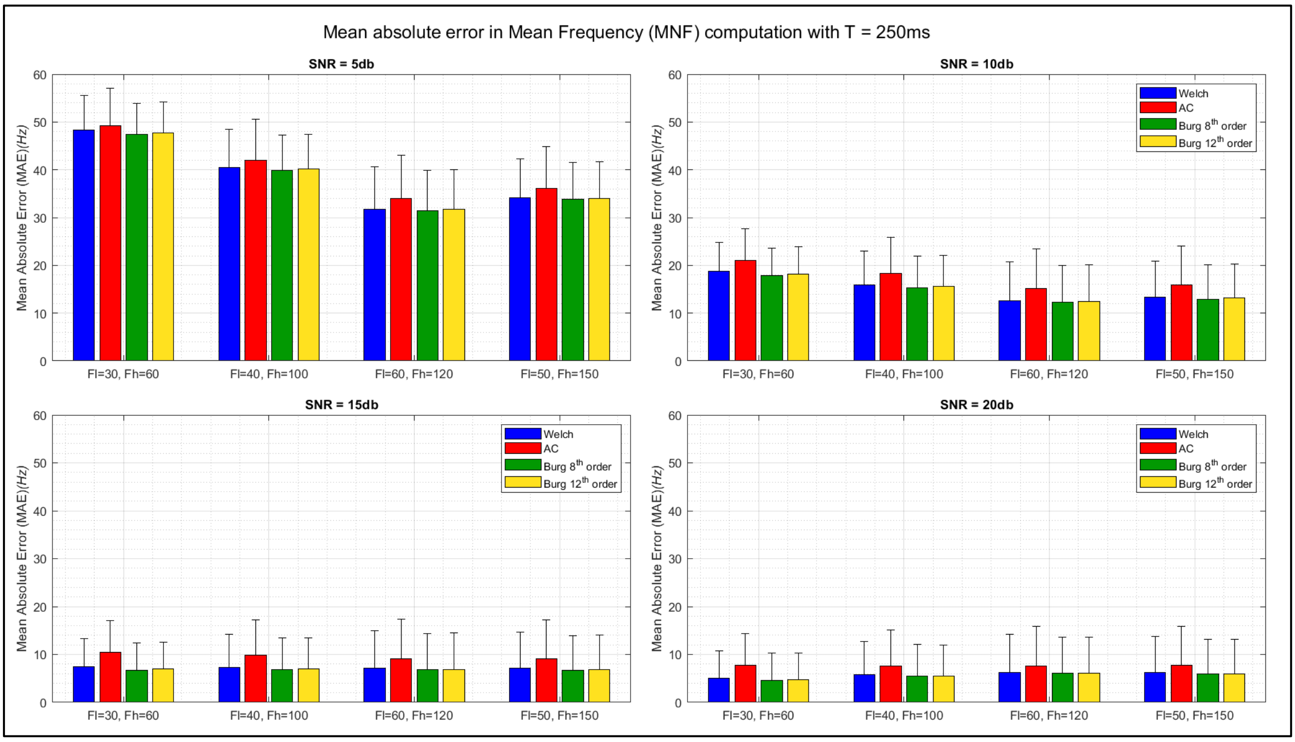

Figure 4 Mean Absolute Error (MAE) computed for Mean Frequency (MNF). Errors were generated by four different cut-off frequencies and analysed at four different level of SNR. The duration of the signal was set to 250ms. The 8th order of AR model produced the minimum error in the MNF estimation (SNR<20dB) with significant difference with the other methods ($p<0.05$), except for 12th Burg's order. By increasing the SNR, the overall error decreased significantly for each method, passing from 31-50*Hz* at SNR = 5dB to 4-8*Hz* at SNR=20dB.

3.3.2 Effect on Median Frequency

Three-way ANOVA test indicated that there was a significant interaction effect among *SNR*, *cut-off*, and *methods*. Two-way ANOVA tests (four tests, each one for a fixed level of *SNR*) exhibited a significant interaction effect ($p<0.001$) between *cut-off* and *method*, as exemplified in table 4.

Table 4 Two-way ANOVA test results: F-statistics and p-values for Mean Absolute Error computed for MDF. Each test was performed fixing one cut-off while considering SNR and method as main factors. The level of significance was set to *p<0.05, **p<0.01 and ***p<0.001.

	SNR=5dB		*SNR=10dB*		*SNR=15dB*		*SNR=20dB*	
	F-statistic	p-value	F-statistic	p-value	F-statistic	p-value	F-statistic	p-value
Cut-off	195.46	0***	189.89	0***	239.87	0***	264.54	0***
Method	112.14	0***	105.27	0***	66.39	0***	53.44	0***
*Cut-off*method*	8.11	0***	6.73	0***	4.88	0***	4.45	0***

For the Median frequency estimation, the *12th order* of the autoregressive model outperformed all the other methods ($p<0.001$) when the power of the spectrum was located at low frequencies (MDF_{ideal}=46.88*Hz*) for SNR less or equal to 15dB. When SNR was equal to 20dB, the *12th order* produced again the minimum error with a significant difference with respect to the other methods ($p<0.001$) except for the *8th order* (not significant). When cut-off was $f_l=40$-$f_h=100$, the 8th order generated the minimum error at each level of SNR and the difference with respect to all the other methods was significant ($p<0.001$), although for low level of SNR (5 and 10dB*)* the difference with the *12th order* was not significant. When cut-off was $f_l=60$-$f_h=120$, the *8th order* of Burg outperformed all the other methods ($p<0.001$) even if the level of significance was lower at higher SNR ($p<0.05$). Lastly, when the power of the spectrum was located at high frequencies (cut-off $f_l=50$-$f_h=150$) the minimum error was always obtained by the *8th order,* with significant difference from the other methods ($p<0.01$ and $p<0.05$) in presence of noisy signals (SNR=5 and 10dB, respectively). When SNR was equal to 15dB, the difference between the *8th order* and *Welch* was not significant anymore. When in presence of high level of SNR (20dB), the 8th order produced again the minimum error and the difference with *12th order* and *Welch* was not significant. The errors are presented in figure 5.

Finally, we found that the error generated by a single method when the frequency content was in the low area (cut-off $f_l=30$-$f_h=60$) was statistically different ($p<0.001$) from the errors computed by the same method but with different frequency content (that is, cut-off $f_l=40$-$f_h=100$, $f_l=50$-$f_h=150$, $f_l=60$-$f_h=120$). This significance was found at all the analyzed level of SNR (from 5 to 20dB) and for each single method separately.

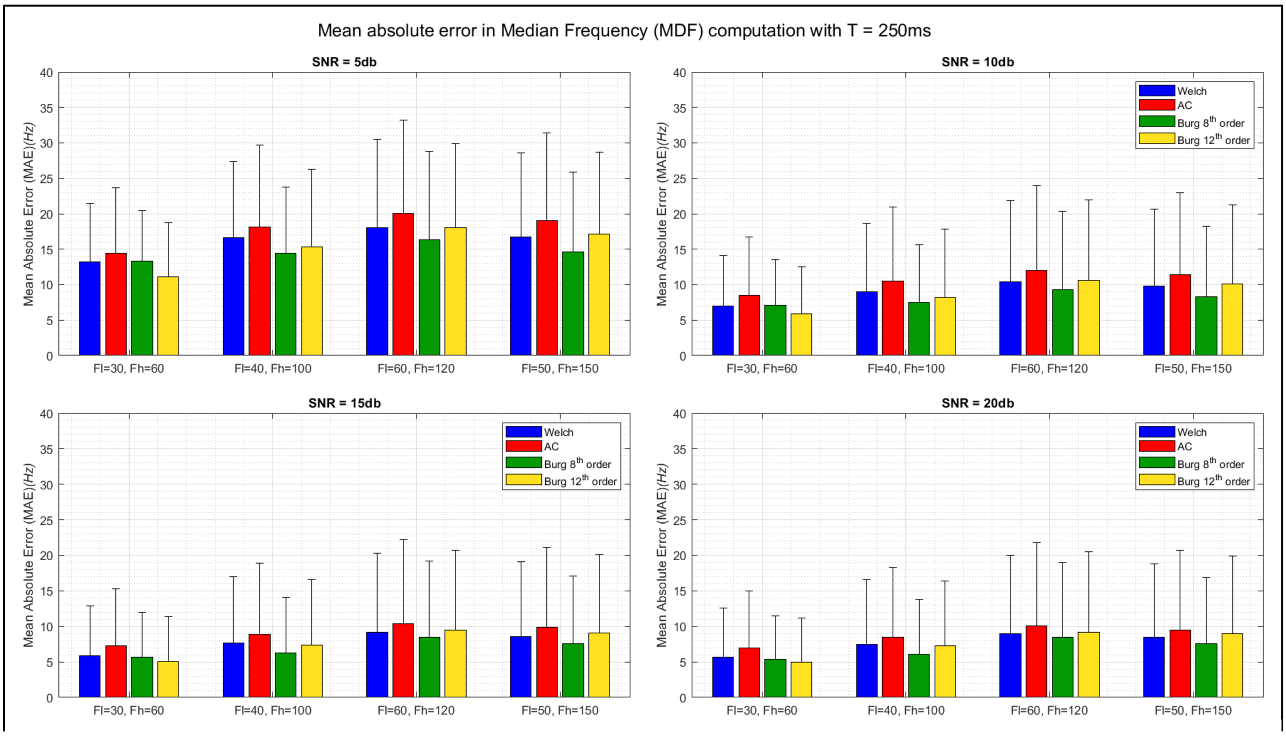

Figure 5 Mean Absolute Error (MAE) computed for Median Frequency (MDF). Errors were generated by four different cut-off frequencies and analyzed at four different level of SNR. The duration of the signal was set to 250ms. The AR model produced the minimum error in the MDF computation in each examined case ($p<0.05$). For cut-off $f_l=30$-$f_h=60$ the *12th order* produced the minimum error, while the *8th order* outperformed the other method in all the other cases (i.e., all the other cut-off frequencies). By increasing the SNR, the overall error decreased significantly for each method, passing from 13-20Hz at SNR = 5dB to 5-10Hz at SNR=20dB.

4. Discussion

From the comparison of window functions for *Welch* method, we noticed that the type of window function slightly influences the PSD estimation. In fact, several windows produced similar results with negligible differences. In general, when the SNR is poor (5 and 10dB), there is not any difference in the selected window because the main effect on estimation performance is driven by the amount of noise. For higher level of SNR

(15 and 20dB), some windows (i.e., Tukey, Taylor, Bartlett et al.) produced significant smaller error because of the variance reduction on the spectral estimation given by the shape of the window. This behavior suggested us to adopt the Tukey window for the performance analysis.

For the analysis of autoregressive model's order, we noticed a different behavior in the computation of Mean Frequency and Median Frequency depending on the frequency location of the power content of the signals. Regarding the MNF, as we increased the order of the AR model, the error slightly increased, despite the difference among errors was not significant after the 7^{th} order. This negative effect is due to an overfitting related to the model estimation; in fact, by increasing the order, it happens that also the noise superposed to the signal is represented and reproduced by the model itself. Therefore, if only the MNF is selected as variable of interest instead of considering both MNF and MDF like in Farina [12], the model's order can be decreased in the range 6^{th} to 8^{th} with respect to the 10^{th} suggested in [12] to reduce the estimation variance and the computation time.

Regarding the Median Frequency computation, the minimum order that produced the smallest error changed according to the level of SNR and the location in which the power of the signal was concentrated. When the value of Median Frequency lied within low frequencies (45-50*Hz*), a high order (around 12-13^{th}) of AR model is required in presence of elevated noise (SNR=5 and 10dB); for higher SNR, the number of required parameters goes down to 11 or 12. Generally, we need a high number of AR model parameters to shape a PSD whose frequency content is not negligible in a low frequency area (0-40*Hz*).

If the ideal value of Median Frequency might be found at high frequencies (90-100*Hz*), as the case analyzed by Farina [farina], a low order is needed because the ideal PSD shape can be approximated by only a few model's parameters (from 6 to 8, depending on the level of noise). Therefore, depending on the frequency location of the signal's power and on the level of noise, the minimum order of the AR model to be used changes.

Finally, by comparing all the methods, we noticed that both *Burg* and *Welch* always outperformed *AC* method, so we recommend no to use this last one. In presence of noise (SNR<20dB), *Burg* showed better result than *Welch*, although the optimum model's order depends on frequency location of the power spectrum and on the level of noise. We suggest using an order of 7-8 as a general rule, if we do not expect a substantial decreasing trend of spectral variables (if muscle fatigue is not expected). If a compression towards lower frequency is expected, we agree with the recommendation of Farina's work to use an order of 10 (even 12 if SNR is very low). In general, if we can ensure high SNR (SNR≥20dB) and we want to investigate non-fatiguing conditions, in which the spectrum is not compressed towards lower frequencies, *Burg* and *Welch* become equivalent in the MNF and MDF estimation.

5. Conclusion

We evaluated the performance of different algorithms at various levels of SNR with special attention to the frequency location of the spectra. The methods were tested on simulated sEMG signals generated with four different frequency contents, simulating different physiological status of a muscle. In fact, during non-fatiguing conditions the frequency content of the spectrum is high (in general in the range 80-120Hz), while in presence of muscle fatigue, we could find spectral compression to low frequency areas (range 40-60Hz). Although many works in recent years focused on the study of myoelectric manifestation of fatigue, no comparison have been performed evaluating the consequences on the performance of the estimation techniques caused by the substantial shift towards lower frequency of the PSD.

For the Welch method, we found that the type of window slightly influences the estimate. Our results suggest choosing the Tukey window as a function to segment the signals. Regarding the Autoregressive model, we found that the error generated in MNF computation is less dependent on the shape of the spectra, and a low order is enough (6^{th}-8^{th}). If MDF should be analyzed, the order must be chosen according to the expected shape of the spectrum and the level of noise. Finally, results suggested that the AR model is more robust in the PSD estimation than all the other methods at each level of SNR for signals of short duration (T=250ms). Moreover, the 8^{th} order provided the best results in most of the cases. In presence of high level of SNR, lower orders might yield better result for non-fatiguing contractions. Nevertheless, if the effects of muscular fatigue, where a considerable compression of the spectrum is expected, a higher order (e.g., 10^{th} or 12^{th}) could better approximate the PSD to the real one in the relevant frequency band.

All the results have been obtained from the analysis of stationary synthetic, although different frequency contents have been examined to reproduce myoelectric manifestation of fatigue. For real experimental signals, it could be useful to develop an adaptive algorithm that automatically select the optimum order of AR model based on the frequency content and SNR level. In this way, AR method could provide optimal results even in the analysis of slow changes that fall within the analyzed signal duration.

References

[1] Merletti, R., Parker, P., 2004. Electromyography: physiology, engineering, and noninvasive applications, IEEE Press series in biomedical engineering. IEEE/John Wiley & Sons, Hoboken, NJ.

[2] Merletti, R., Muceli, S., 2019. Tutorial. Surface EMG detection in space and time: Best practices. J.Electromyogr.Kines. 49, 102363. https://doi.org/10.1016/j.jelekin.2019.102363

[3] Cifrek, M., Medved, V., Tonković, S., Ostojić, S., 2009. Surface EMG based muscle fatigue evaluation in biomechanics. Clinical Biomechanics 24, 327–340. https://doi.org/10.1016/j.clinbiomech.2009.01.010

[4] Nazmi, N., Abdul Rahman, M., Yamamoto, S.-I., Ahmad, S., Zamzuri, H., Mazlan, S., 2016. A Review of Classification Techniques of EMG Signals during Isotonic and Isometric Contractions. Sensors 16, 1304. https://doi.org/10.3390/s16081304

[5] Phinyomark, A., Thongpanja, S., Hu, H., Phukpattaranont, P., Limsakul, C., 2012. The Usefulness of Mean and Median Frequencies in Electromyography Analysis, in: Naik, G.R. (Ed.), Computational Intelligence in Electromyography Analysis - A Perspective on Current Applications and Future Challenges. InTech. https://doi.org/10.5772/50639

[6] Shair, E.F., Ahmad, S.A., Marhaban, M.H., Mohd Tamrin, S.B., Abdullah, A.R., 2017. EMG Processing Based Measures of Fatigue Assessment during Manual Lifting. BioMed Research International 2017, 1–12. https://doi.org/10.1155/2017/3937254

[7] Hof, A.L., 1991. Errors in frequency parameters of EMG power spectra. IEEE Transactions on Biomedical Engineering 38, 1077–1088. https://doi.org/10.1109/10.99071

[8] Merletti, R., Balestra, G., Knaflitz, M., 1989. Effect of FFT based algorithms on estimation of myoelectric signal spectral parameters, in: Images of the Twenty-First Century. Proceedings of the Annual International Engineering in

Medicine and Biology Society,. Presented at the Images of the Twenty-First Century. Proceedings of the Annual International Engineering in Medicine and Biology Society, pp. 1022–1023 vol.3. https://doi.org/10.1109/IEMBS.1989.96066

[9] Karlsson, S., Yu, J., Akay, Y., 2000. Time-frequency analysis of myoelectric signals during dynamic contractions: A comparative study. IEEE transactions on bio-medical engineering 47, 228–38. https://doi.org/10.1109/10.821766

[10] Bonato, P., Roy, S.H., Knaflitz, M., de Luca, C.J., 2001. Time-frequency parameters of the surface myoelectric signal for assessing muscle fatigue during cyclic dynamic contractions. IEEE Trans. Biomed. Eng. 48, 745–753. https://doi.org/10.1109/10.930899

[11] Mañanas, M.A., Jané, R., Fiz, J.A., Morera, J., Caminal, P., 2002. Influence of estimators of spectral density on the analysis of electromyographic and vibromyographic signals. Med. Biol. Eng. Comput. 40, 90–98. https://doi.org/10.1007/BF02347701

[12] Farina, D., Merletti, R., 2000. Comparison of algorithms for estimation of EMG variables during voluntary isometric contractions. Journal of Electromyography and Kinesiology 10, 337–349. https://doi.org/10.1016/S1050-6411(00)00025-0

[13] Keller, J.L., Housh, T.J., Camic, C.L., Bergstrom, H.C., Smith, D.B., Smith, C.M., Hill, E.C., Schmidt, R.J., Johnson, G.O., Zuniga, J.M., 2018. The effect of epoch length on time and frequency domain parameters of electromyographic and mechanomyographic signals. Journal of Electromyography and Kinesiology 40, 88–94. https://doi.org/10.1016/j.jelekin.2018.04.003

[14] Clancy, E.A., Farina, D., Merletti, R., 2005. Cross-comparison of time- and frequency-domain methods for monitoring the myoelectric signal during a cyclic, force-varying, fatiguing hand-grip task. Journal of Electromyography and Kinesiology 15, 256–265. https://doi.org/10.1016/j.jelekin.2004.11.002

[15] Zhang, Z.G., Liu, H.T., Chan, S.C., Luk, K.D.K., Hu, Y., 2010. Time-dependent power spectral density estimation of surface electromyography during isometric muscle contraction: Methods and comparisons. Journal of Electromyography and Kinesiology 20, 89–101. https://doi.org/10.1016/j.jelekin.2008.09.007

[16] Rampichini, S., Vieira, T.M., Castiglioni, P., Merati, G., 2020. Complexity Analysis of Surface Electromyography for Assessing the Myoelectric Manifestation of Muscle Fatigue: A Review. Entropy 22, 529. https://doi.org/10.3390/e22050529

[17] Cao, L., Wang, Y., Hao, D., Rong, Y., Yang, L., Zhang, S., Zheng, D., 2017. Effects of Force Load, Muscle Fatigue, and Magnetic Stimulation on Surface Electromyography during Side Arm Lateral Raise Task: A Preliminary Study with Healthy Subjects. BioMed Research International 2017, e8943850. https://doi.org/10.1155/2017/8943850

[18] Puce, L., Pallecchi, I., Marinelli, L., Mori, L., Bove, M., Diotti, D., Ruggeri, P., Faelli, E., Cotellessa, F., Trompetto, C., 2021. Surface Electromyography Spectral Parameters for the Study of Muscle Fatigue in Swimming. Front. Sports Act. Living 3, 644765. https://doi.org/10.3389/fspor.2021.644765

[19] Karthick, P.A., Venugopal, G., Ramakrishnan, S., 2015. Analysis of surface emg signals under fatigue and non-fatigue conditions using b-distribution based quadratic time frequency distribution. J. Mech. Med. Biol. 15, 1540028. https://doi.org/10.1142/S021951941540028X

[20] González-Izal, M., Malanda, A., Gorostiaga, E., Izquierdo, M., 2012. Electromyographic models to assess muscle fatigue. Journal of Electromyography and Kinesiology 22, 501–512. https://doi.org/10.1016/j.jelekin.2012.02.019

[21] Stulen, F.B., De Luca, C.J., 1981. Frequency Parameters of the Myoelectric Signal as a Measure of Muscle Conduction Velocity. IEEE Trans. Biomed. Eng. BME-28, 515–523. https://doi.org/10.1109/TBME.1981.324738

[22] Rinaldi, M., D'Anna, C., Schmid, M., Conforto, S., 2018. Assessing the influence of SNR and pre-processing filter bandwidth on the extraction of different muscle co-activation indexes from surface EMG data. Journal of Electromyography and Kinesiology 43, 184–192. https://doi.org/10.1016/j.jelekin.2018.10.007

[23] Wiener, N., 1930, Generalized Harmonic Analysis, Acta Mathematica. 55:117-258. doi:10.1007/bf02546511

[Signals and Systems for Bioengineers (Second Edition)].

[24] Welch, P., 1967, The use of fast Fourier transform for the estimation of power spectra: A method based on time averaging over short, modified periodograms, IEEE Transactions on Audio and Electroacoustics 15 (2), pp. 70-73, doi: 10.1109/TAU.1967.1161901.

[25] Bartlett, M.S., 1950, Periodogram analysis and continous spectra, Biometrika 37, Issue 1-2, pp. 1-16, https://doi.org/10.1093/biomet/37.1-2.1

[26] Burg, J.P., 1967, Maximum Entropy Spectral Analysis, Proceedings of 37th Meeting, Society of Exploration Geophysics, Oklahoma City.

[27] R Core Team, 2021, R: A language and environment for statistical computing. R Foundation for Statistical Computing, Vienna, Austria. URL http://www.R-project.org/.

Appendix A

In this paragraph, the mathematical formulation of all utilized window functions is presented.

1- Bartlett,

$$w(n) = \begin{cases} 2n/N, & 0 \le n \le \frac{N}{2} \\ 2 - 2n/N, & \frac{N}{2} \le n \le N \end{cases} \quad \text{(A.1)}$$

2- Barthann,

$$w(n) = 0.62 - 0.48|n/N - 0.5| + 0.38\cos\left(2\pi(n/N - 0.5)\right) \qquad 0 \le n \le N \quad \text{(A.2)}$$

3- Blackman,

$$w(n) = 0.42 - 0.5\cos\left(\frac{2\pi n}{N-1}\right) + 0.08\cos\left(\frac{4\pi n}{N-1}\right) \qquad 0 \le n \le N-1 \quad \text{(A.3)}$$

4- Blackmanharris,

$$w(n) = 0.358 - 0.488\cos\left(\frac{2\pi n}{N-1}\right) + 0.141\cos\left(\frac{4\pi n}{N-1}\right) - 0.011cos\left(\frac{6\pi n}{N-1}\right) \qquad 0 \le n \le N-1 \quad \text{(A.4)}$$

5- Chebyshev,

$$w(n) = \left\{\cos\left[\frac{N}{\cos\left[\alpha\cos\left(\frac{\pi m}{n}\right)\right]}\right]\right\} \Big/ \left\{\cosh\left[\frac{N}{cosh(\alpha)}\right]\right\} \qquad 0 \le n \le N-1 \quad \text{(A.5)}$$

With $\alpha = \cosh\left((1/N)/cosh\,(10\hat{}\gamma\,)\,\right)$

6- Flattop,

$$w(n) = 0.215 - 0.416\cos\left(\frac{2\pi n}{N-1}\right) + 0.277\cos\left(\frac{4\pi n}{N-1}\right) - 0.083cos\left(\frac{6\pi n}{N-1}\right) + 0.006\cos\left(\frac{8\pi n}{N-1}\right) \qquad 0 \le n \le N-1 \quad \text{(A.6)}$$

7- Gaussian,

$$w(n) = \exp^{-\frac{1}{2}\left(\alpha\frac{n}{(N-1)/2}\right)} = e^{-n^2/2\sigma^2} \qquad 0 \le n \le N-1 \qquad \text{(A.7)}$$

8- Hamming,

$$w(n) = 0.54 - 0.46\cos\left(\frac{2\pi n}{N}\right) \qquad 0 \le n \le N \qquad \text{(A.8)}$$

9- Hann,

$$w(n) = 0.5\left(1 - \cos\left(\frac{2\pi n}{N}\right)\right) \qquad 0 \le n \le N \qquad \text{(A.9)}$$

10- Kaiser,

$$w(n) = \frac{I_0\left(\beta\sqrt{1-\left(\frac{n-N/2}{N/2}\right)^2}\right)}{I_0(\beta)} \qquad 0 \le n \le N \qquad \text{(A.10)}$$

$$\beta = \begin{cases} 0.11(\alpha - 8{,}7), & a > 50 \\ 0.584(\alpha-21)^2 + 0.078(\alpha - 21), & 50 \ge a \ge 21 \\ 0, & a < 21 \end{cases}$$

11- Nuttal

$$w(n) = 0.363 - 0.489\cos\left(\frac{2\pi n}{N-1}\right) + 0.136\cos\left(\frac{4\pi n}{N-1}\right) - 0.010 cos\left(\frac{6\pi n}{N-1}\right) \qquad 0 \le n \le N-1 \qquad \text{(A.11)}$$

12- Parzen,

$$\begin{cases} 1 - 6\left(\frac{|n|}{N/2}\right)^2 + 6\left(\frac{|n|}{N/2}\right)^3, & 0 \le |n| \le (N-1)/4 \\ 2 - \frac{2n}{N}, & (N-1)/4 \le n \le (N-1)/2 \end{cases} \qquad \text{(A.12)}$$

13- Rectangular,

$$w(n) = 1 \qquad 0 \le n \le N \qquad \text{(A.13)}$$

14- Taylor

$$w(n) = 1 + 2\sum_{m=1}^{n-1} F_m \cos\left[\frac{2\pi m(n - N/2 + 1/2)}{N}\right] \qquad 0 \le n \le N-1 \qquad \text{(A.14)}$$

$$F_m = \left\{(-1)^{(m+1)} \prod_{i=1}^{\bar{n}-1} \left[1 - \frac{m^2/\sigma^2}{[(\ln{(B+\sqrt{(B^{\wedge}2\,)-1})}/\pi]^2 + (i-1/2)^2}\right]\right\} \Big/ \left\{2 \prod_{j=1, j\neq m}^{\bar{n}-1} (1 - \frac{m^2}{j^2})\right\}$$

With $B = 10^{-\frac{SLL}{20}}, \bar{n}$ is the number of nearly constant level sidelobes adjacent to the main lobe, SLL is the peak sidelobe level (in dB) relative to the main lobe peak.

15- Triangular,

$$w(n) = \begin{cases} \dfrac{2n}{N+1} & 1 \leq n \leq (N+1)/2 \\ 2 - \dfrac{2n}{N+1} & (N+1)/2 + 1 \leq n \leq N \end{cases} \quad \text{With N odd}$$

(A.15)

$$w(n) = \begin{cases} \dfrac{(2n-1)}{N+1} & 1 \leq n \leq N/2 \\ 2 - \dfrac{(2n-1)}{N+1} & N/2 + 1 \leq n \leq N \end{cases} \quad \text{With N even}$$

16- Tukey

$$w(n) = \begin{cases} \dfrac{1}{2}\left\{1 + \cos\left(\dfrac{2\pi}{r}[x - r/2]\right)\right\}, & 0 \leq n \leq r/2 \\ 1, & r/2 \leq n \leq 1 - r/2 \\ \dfrac{1}{2}\left\{1 + \cos\left(\dfrac{2\pi}{r}[x - 1 + r/2]\right)\right\}, & 1 - r/2 \leq n \leq 1 \end{cases} \tag{A.16}$$

with r is the ratio of cosine-tapered section length to the entire window length with $0 \leq r \leq 1$.